 

# Photochemical Synthesis of Nonlinear Optical and Photorefractive Materials

*Anatoly V. Vannikov[1], Antonina D. Grishina[1], Larisa Ya. Pereshivko[1], Tatjana V. Krivenko[1], and Rodney W. Rychwalski[2]*
*[1]A.N. Frumkin Inst. of Electrochemistry, Russian Aca. of Science, Moscow, Russia*
*[2]Department of Polymeric Materials, Chalmers Univ. of Tech., Göthenburg, Sweden*

## Abstract

Photochemical formation of image with nonlinear optical and photorefractive properties in polymer layers is displayed. The layers were obtained using composition of polyhydroxyaminoether containing aromatic amino groups in polymer chains and tetrabromomethane. Donor-acceptor complexes form in the layers and irradiation of the layers by light in the range 330-450 nm stimulates electron transfer from the donor to the acceptor leading to the synthesis of colored polycation product which possesses the nonlinear optical and charge carrier photo-generating properties. Besides, these layers are electron-transporting ones. All of it allowed to obtain light-sensitive layers for recording nonlinear optical and photorefractive images and patterns.

## Introduction

In the present paper the possibility of photochemical synthesis of photorefractive (PF) medium is demonstrated. Initial layer is a composition of polyhydroxyaminoether (PHAE) with a donor aromatic amino-groups (Am) in the main chain and the acceptor tetrabromomethane ($CBr_4$). In this composition the donor-acceptor complex Am•$CBr_4$ is formed the excitation of which (light in the range of 330 - 500 nm) gives rise to the electron transfer from amine group to acceptor followed by the formation of polycationic chromophore[1] according to the Scheme 1:

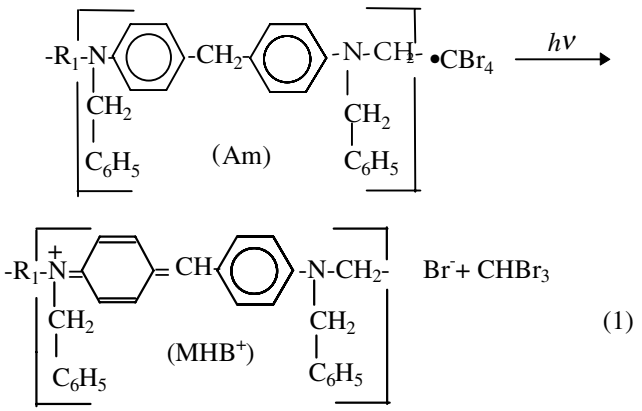


(1)

where $R_1$ is ether-group responsible for adhesion, flexibility and other useful properties of the polymer. The chromophore fragment structure is similar to Michler's hydrol blue ($MHB^+$) one.

## Experiment and Results

The PHAE absorption has a long-wavelength threshold at 370 nm. The $CBr_4$ added displaces this threshold to 500 nm due to the formation of Am•$CBr_4$ charge-transfer complex.

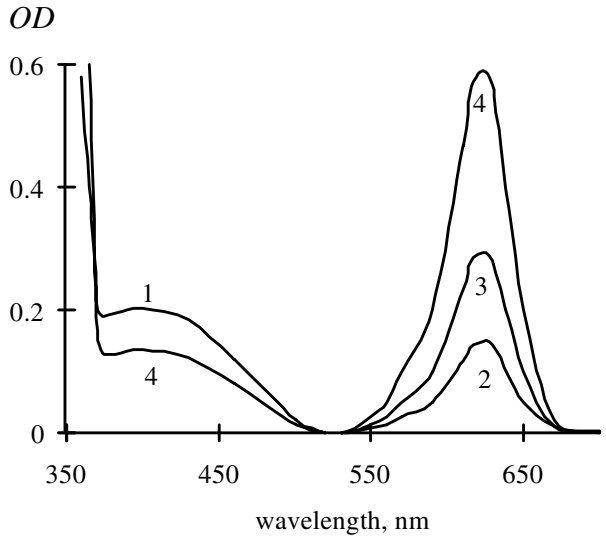


*Figure 1. Spectral dependence of optical density (OD). Exposure dose at 365 nm, mJ/cm²: 0 (1), 75 (2), 150 (3) and 300 (4).*

As is shown in Fig.1, under the action of the light of 365 nm, there appears an additional band with maximum at 630 nm connected with the formation of the $MHB^+$-like fragment in the main chain according to Scheme (1). Fig.1 shows that the $MHB^+Br^-$ fragment absorbs light in the range of 600 - 700 nm, a maximum being at 630 nm. As follows from date in Fig. 1, absorbance at the maximum linearly increases from 0 to 0.5 with increasing exposure to 300 mJ/cm². Quantum yield of the $MHB^+$ $Br^-$ chromophore formation is approximately 0.12. After fixation of the

exposed layer by means of moving away (heating to 80°C) $CBr_4$ that has not reacted with amine groups, unexposed areas contain only PHAE and exposed ones consist of the PHAE containing the $MHB^+$ $Br^-$ chromophores in main chain.

Photochemical formation of the $MHB^+Br^-$ cromophores leads to manifestation of nonlinear optical (NLO) properties, namely second harmonic generation[2] (SHG). The SH intensity linearly increases with increasing the $MHB^+Br^-$ concentration. To understand mechanism of SHG it were estimated dipole moments of the $MHB^+$ fragment in ground and first excited states. The $MHB^+$ is bond-equivalent symmetrical fragment. In according to notion[3] the geometry optimization of structure $MHB^+$ $Br^-$ consisting of the conjugated cation and point counter anion was realized. In this geometry, the estimated dipole moments for the $MHB^+$ ground and first excited states are equal to 7.5 D and 1.5 D, accordingly. Thus, the $Br^-$ counter anion induces the bond-length alternation of the $MHB^+$ cation and, hence, produces the molecular second-order nonlinearity and causes SHG. The resulting NLO polarizability is similar with that of for donor/acceptor NLO systems.

It is known as well that the exposed areas of PHAE have photoelectric sensitivity to a laser beam[4]. Photoexcitation of $MHB^+Br^-$ in the wavelength range of 600 - 700 nm induces electron transfer according to the Scheme:

$$(MHB^+\ Br^-) \xrightarrow{h\nu} (MHB^+\ Br^-)^* + Am \rightarrow$$

$$MHB^{\bullet}\ Br^- + Am^{+\bullet} \qquad (2)$$

followed by the formation of trapped electron and mobile hole $Am^{+\bullet}$:

$$Am + Am^{+\bullet} \rightarrow Am^{+\bullet} + Am \qquad (3)$$

that is multiple electron transfer from the neutral Am group to the radical cation $Am^{+\bullet}$. The measurements of drift mobility $\mu$ were performed by the known time-of-flight method. By thermal evaporation in vacuum the generation layer of Se was coated onto the free surface of polymer film and then the semitransparent gold electrode was applied. The charge carriers were generated in Se by laser pulse. The temperature and electric field dependences of $\mu$ obey Gill's equation and, for example at room temperature for $OD(647) = 0.4$ and $E_0 = 5\ 10^5$ V/cm $\mu = 2.4\ 10^{-6}$ $cm^2$/V s, sharply decreasing as $E_0$ diminishes.

Fig. 2 shows the increase of $(J_{ph} + J_d)/J_d$ at exposing by laser beam with $\lambda = 647$ nm and its decay after laser beam switching off for the sample having $MHB^+$ optical density $OD(647) = 0.08$, $J_{ph}$ and $J_d$ being photo and dark current correspondingly.

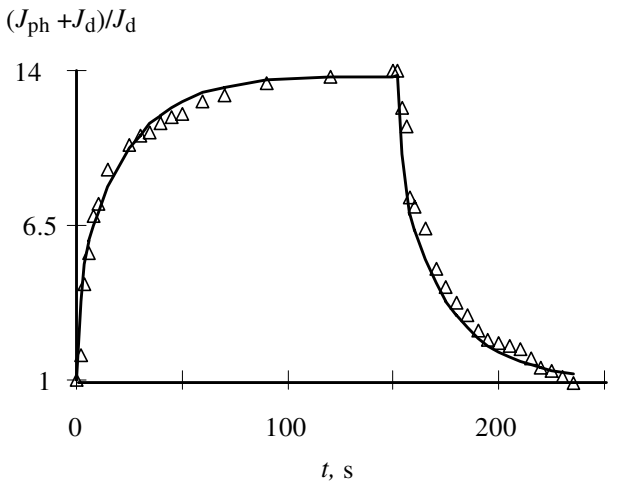


*Figure 2. Photocurrent dependence on time. At t = 0 laser beam is switched on, at $t_1$ =150 s it is switched off.*

The photo- and dark current measurements were carried out for the layers cast onto a quartz substrate with a photolithographically prepared meander of two Cr-Ni electrodes. Spacing between electrode was 40 μm, electric field $E_0 = 8$ V/μm. The sample was irradiated by laser beam of the intensity 720 mW/$cm^2$. The experimental data in Fig. 1 are well fit with the double exponential (solid curves):

$$(J_{ph}+J_d)/J_d = 14 - 9\ EXP(-t/24) - 4\ EXP(-t/2) \qquad (4)$$

for the photocurrent at exposing and

$$(J_{ph} + J_d)/J_d = 1 + 9EXP[-(t - t_1)/24] + 4\ EXP[-(t - t_1)/2] \qquad (5)$$

for the current after laser beam switching off at $t_1$.

Fig. 3 shows the dependence of the dark current and $(J_{phm})/J_d$ ($J_{phm}$ is a maximum photocurrent) on $OD(647)$.

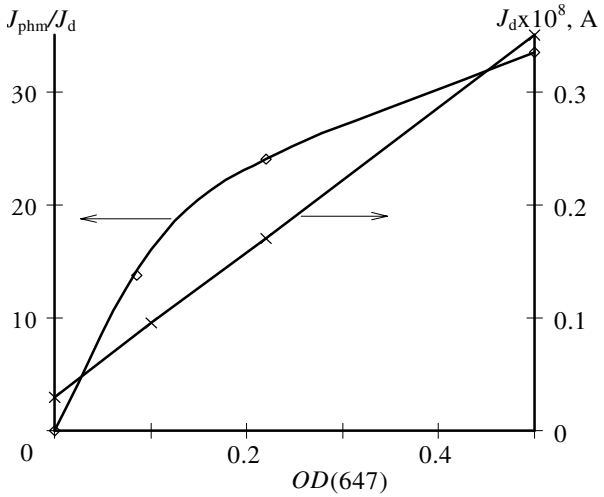


*Figure 3. Dependence of dark current and steady-state photo-current on OD(647)*

So, the layers obtained by photochemical modification of the PHAE-$CBr_4$ composition posses the photoelectric and NLO properties which are necessary for photorefractive effect.

The two-beam coupling technique was used to characterize PR effect. Two coherent writing *p*-polarized beams were overlapped in the layer to create a fringe pattern. The transmission of the two writing beams was measured, giving the diffraction efficiency $\eta$, the amplification factor $\gamma_0$ and the gain coefficient $\Gamma$. The intensity of each writing beam (Ar-Kr-laser, $\lambda$ = 647 nm) was 720 mW/cm$^2$. The tilt angle was $\theta = 45^\circ$ and angle between two beams was 15° in air. In order to orient the initially randomly distributed $MHB^+$ and to obtain macroscopic second-order properties an external electric field $E_0$ = 8 V/μm was applied using the corona discharge technique. Optical density of the layer at 647 nm proportional to concentration of the photochemically formed $MHB^+$ was *OD*(647) = 0.08, 0.2 and 0.4 for different samples with thickness $d$ = 30 μm and 7.4 μm.

Fig. 4 shows results of three separate experiments for the sample with *OD*(647) = 0.08. In the first experiment (a beam ratio before the sample $\beta = I_1(0)/I_2(0) = 1$), the beam 1 intensity (curve 1) is measured as beam 2 is switched on at $t$ = 20 s (arrow up) and switched off at $t$ = 140 s (arrow down).

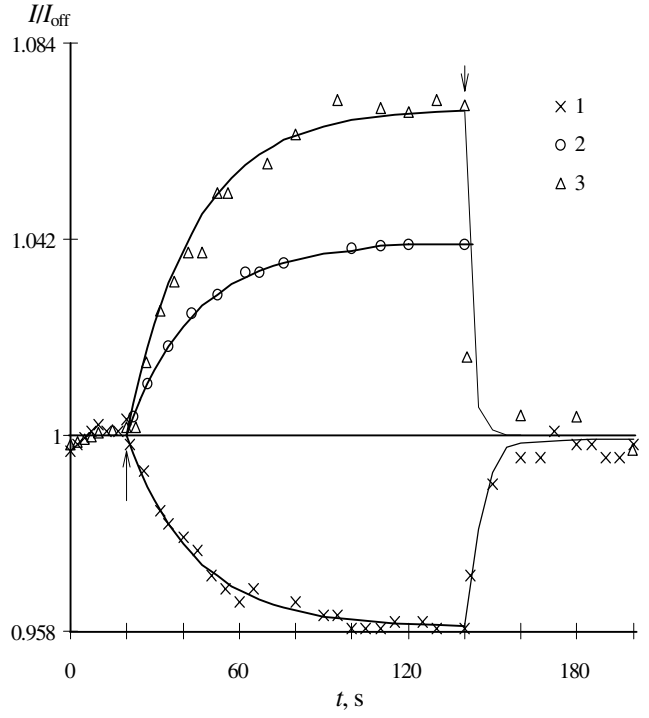


*Figure 4. Three separate two-beam-coupling experiments for sample having OD(647) = 0.08. The intensity of beam 1 (1) is measured at $\beta$ = 1 as beam 2 is switched on (arrow up) and off (arrow down). The intensity of beam2 is measured at $\beta$ = 1 (2) and 2.36 (3) as beam1 is switched on and off.*

In the second experiment, the intensity of beam 2 (curve 2) is measured at $\beta = 1$ as beam 1 is switched on at $t$ = 20 s and switched off at $t$ = 140 s. The third experiment (curve 3) is the same as the second one, only $\beta = 2.36$. Time $t = 0$ corresponds to the moment of simultaneous switching on of one of the beams and the corona. It is seen in Fig. 4, that as the grating is written the intensity of beam 1 decreases and intensity of beam 2 increases by approximately equal quantity, indicating on index-of-refraction grating shifted relative to the light intensity grating.

Fig. 4 shows that the experimental data are well fit with the expressions:

$$I_1/I_{1off} = 1 - 0.041[1 - EXP[-(t - 20)/24] \quad (6)$$

solid curve 1,

$$I_2/I_{2off} = 1 + 0.041[1 - EXP[-(t - 20)/24] \quad (7)$$

solid curve 2 for $\beta = 1$ and

$$I_2/I_{2off} = 1 + 0.07[1 - EXP[-(t - 20)/24] \quad (8)$$

solid curve 3 for $\beta = 2.36$, where $I_{1off}$ is the intensity of beam 1 at the blocked beam 2 and $I_{2off}$ is the intensity of beam 2 at the blocked beam 1. After steady state transfer was achieved, the amplification factor $\gamma_0$ was measured and, for example, for $\beta = 1$, $\gamma_0 = I_2/I_{2off} = 1.041$.

Table 1 summarizes the PR properties of the studied materials**.**

**Table 1. Photorefractive characteristics of the studied layers**

| | $d$, μm | $\gamma_0$ | $\alpha L$ | $\Gamma L$ | $\eta$% | $\Gamma$, cm$^{-1}$ |
|---|---|---|---|---|---|---|
| *OD*=0.08 | 30 | | 0.2 | | | |
| $\beta = 1$ | | 1.041 | | 0.082 | 0.17 | 24.6 |
| $\beta = 2.36$ | | 1.07 | | 0.098 | 0.24 | 29.4 |
| *OD* = 0.2 | 30 | | 0.51 | | | |
| $\beta = 1$ | | 1.05 | | 0.100 | 0.25 | 30 |
| $\beta$ =4.24 | | 1.15 | | 0.176 | 0.77 | 52.8 |
| *OD* = 0.4 | 7.4 | | 0.92 | | | |
| $\beta$ =1 | | 1.06 | | 0.120 | 0.36 | 162.4 |
| $\beta$ =4.4 | | 1.1 | | 0.118 | 0.35 | 160 |
| $\beta$ =12 | | 1.15 | | 0.152 | 0.58 | 206 |
| $\beta$ =22 | | 1.32 | | 0.292 | 2.1 | 395 |

Experimental conditions, namely $\beta$ at different *OD*(647), the sample thickness $d$ and also the two-beam coupling ratio $\gamma_0$ are shown in columns 1 - 3, respectively. The two-beam coupling gain coefficient $\Gamma$ is given by $\Gamma = L^{-1}$ [ln($\gamma_0$ $\beta$) - ln(1 + $\gamma_0$ - $\beta$)]. Columns 4 and 5 show products $\alpha L$ = *OD'*/log*e* where $\alpha$ is absorption coefficient $\Gamma L$. Diffraction

efficiency $\eta = \sin^2(\Gamma L/2)$ (column 6). The optical path $L$ and optical density along the optical path ($OD$') for the beam with gain are given by: $L = d/\cos\theta$, $OD'/\cos\theta$.

Table shows that the PR effect was also measured in a wide range of variation of $\beta$ for the samples with $OD(647)$ = 0.4 and thickness 7.4 μm. These results was obtained as follows. Firstly, the kinetic curves of the beam 1 decay is monitored as beam 2 is switched on for $\beta = 1$, that is similar to Fig. 4. Then the beam 2 amplification is monitored as beam 2 is switched on for $\beta = 1$, 4.4, 12 and 22. As shown in Table, as the intensity of beam 2 decreases so that $\beta$ becomes equal to 22, $\gamma_0 = 1.32$ is achieved. The time constant of increasing (or decreasing) of one beam, as the other is switched on, is equal to 24 s independently of the $OD$ value and agrees within the experimental error with the time constant of photocurrent. Therefore, the transport and capture of charge carriers is the factor limiting photorefractive speed in these materials.

## Conclusion

The considered materials and the method of their preparation are distinguished by the possibility (1) to uninterruptedly change the concentration of the NLO and photogenerating sites $MHB^+ Br^-$, (2) to have simultaneously transport ($Am^{+\bullet}$), NLO and charge-generating sites in main polymer chains, (3) to form photographic image with the PR and NLO properties in the polymer layer. We believe that the use of the photo-modified PHAE layers sandwiched between two glass plates coated with ITO rather than charging of the layers with corona discharge will allow to considerably increase $E_0$ and therefore to improve photorefractive characteristics.

## Acknowledgment

We gratefully acknowledge the grant from the International Science and Technology Center (project No. 872-98), the grant from the Royal Swedish Academy of Science (project No. 1337) and the grant from the Russian Foundation for Basic Research (project No. 99-03-32111).

## References

1. A. V. Vannikov, A D. Grishina, M. G. Tedoradze, L. I. Kostenko, A. V. Anikeev and I. V. Koblik, J. Mater.Chem., 3, 761 (1993).
2. A. D. Grishina, L. Ya. Pereshivko, T. V. Krivenko, V. V. Savelyev, E. I. Mal'tsev and A. V. Vannikov, Proceedings of SPIE, Organic Nonlinear Optical Materials, M.Eich, M.G.Kuzyk, eds, 3796,. pg.308. (1999).
3. C. B. Gorman, and S. R. Marder, Proc. Natl. Acad. Sci. USA, 90, 11297, (1993)..
4. A. V. Vannikov, in: ICTS'94 The Physical and Chemistry of Imaging Systems, IS&T's 47 Annual Conference. Final Program and Advance Printing of Papers: 783 (1994).

## Biography

Anatoly Vannikov was graduated from the Moscow State University in 1959. Ph.D. (1965), Doctor of science degree in physical chemistry (1975), professor of physical chemistry (1978). Head of the Laboratory of charge transfer processes (from 1975), Deputy Director of Frumkin Institute of Electrochemistry of Russian Academy of Sciences (from 1983). He is a member of IS&T and SPIE. Scope of activity: electrophysics of organic dielectrics, semiconductors and metals, photochemistry and radiation chemistry of polymer systems, non-silver organic polymer photographic systems, non-linear optical organic systems, polyfunctional polymers.